

General Disclaimer

One or more of the Following Statements may affect this Document

- This document has been reproduced from the best copy furnished by the organizational source. It is being released in the interest of making available as much information as possible.
- This document may contain data, which exceeds the sheet parameters. It was furnished in this condition by the organizational source and is the best copy available.
- This document may contain tone-on-tone or color graphs, charts and/or pictures, which have been reproduced in black and white.
- This document is paginated as submitted by the original source.
- Portions of this document are not fully legible due to the historical nature of some of the material. However, it is the best reproduction available from the original submission.

**NASA
Technical
Memorandum**

NASA TM-86471

ESTIMATING SUNSPOT NUMBER

By Robert M. Wilson, Edwin J. Reichmann
and Dieter L. Teuber

Space Science Laboratory

October 1984

(NASA-TM-86471) ESTIMATING SUNSPOT NUMBER
(NASA) 24 p HC A02/MF A01 CSCL 03B


N85-10896

Unclas
G3/92 24192



National Aeronautics and
Space Administration

George C. Marshall Space Flight Center

1. Report No. NASA TM-86471		2. Government Accession No.		3. Recipient's Catalog No.	
4. Title and Subtitle Estimating Sunspot Number				5. Report Date October 1984	
				6. Performing Organization Code	
7. Author(s) Robert M. Wilson, Edwin J. Reichmann, and Dieter L. Teuber*				8. Performing Organization Report No.	
9. Performing Organization Name and Address George C. Marshall Space Flight Center Marshall Space Flight Center, Alabama 35812				10. Work Unit No.	
				11. Contract or Grant No.	
12. Sponsoring Agency Name and Address National Aeronautics and Space Administration Washington, D.C. 20546				13. Type of Report and Period Covered Technical Memorandum	
				14. Sponsoring Agency Code	
15. Supplementary Notes Prepared by Space Science Laboratory, Science and Engineering Directorate. *Teledyne Brown Engineering, Huntsville, Alabama 35805.					
16. Abstract Using a 3-component sinusoidal fit of \bar{R}_{MAX} versus sunspot cycle number (where \bar{R}_{MAX} is the smoothed sunspot number at cycle maximum) for cycles 8 through 20, considered to be the most reliably known cycles, values of \bar{R}_{MAX} are projected for cycles 21 and 22. For cycle 21, the fit projects an \bar{R}_{MAX} value of 160.5, which compares very well to the actually observed value of 164.5. For cycle 22, it projects an \bar{R}_{MAX} value near 110. Results of linear regression analysis, based on comparisons to observed values of \bar{R}_{MAX} , are presented which allow for a determination of a number of cycle-related parameters, including ASC, DES, MIN-MIN PERIOD, \bar{R}_{MEAN} , SLOPE _{ASC} , and SLOPE _{DES} (defined in the text). It is noted that sunspot cycles can be divided, according to their minimum-to-minimum cycle duration, into two distinct groupings: (1) short-period cycles having a mean cycle duration of about 122 months (ranging between 116 and 126 months) and (2) long-period cycles having a mean cycle duration of about 140 months (ranging between 134 and 149 months). Short-period cycles often are observed as high-valued \bar{R}_{MAX} cycles (4 of 6, with all cycles having $\bar{R}_{MAX} \geq 142$ being short-period cycles, 3 of 3), while long-period cycles often are observed as low-valued \bar{R}_{MAX} cycles (5 of 7). This paradigm relating cycle amplitude to period (observable in 8 of the 13 modern cycles) suggests that cycle 21, being a high-valued \bar{R}_{MAX} cycle (and with $\bar{R}_{MAX} \geq 142$), may also be a cycle of short duration. If so, then cycle 21 will end about August 1986. In contrast to this, however, a plot of MIN-MIN PERIOD versus sunspot cycle number, based on cycles 8 through 20, suggests that cycle 21 may be a cycle of long duration. Consequently, \bar{R}_{MIN} occurrence for cycle 22 would be delayed until about February 1988. Since cycle 22 is projected to be a low-valued \bar{R}_{MAX} cycle with a value very near the observed value for cycle 20, the cycle is expected to be of long duration. Consequently, cycle 22 should peak about October 1990 and end about April 1998, if cycle 21 is a short-period cycle ending about August 1986, or cycle 22 should peak about April 1992 and end about October 1999, if cycle 21 is a long-period cycle. [Two additional, but less likely, predictions must also be noted. These include: (1) if cycle 21 is a long-period cycle and cycle 22 a short-period cycle, then cycle 22 should peak about October 1991 and end about February 1998; and (2) if cycle 21 is a short-period cycle and cycle 22 a short-period cycle, then cycle 22 should peak about April 1990 and end about August 1996.] Using SLOPE _{ASC} and SLOPE _{DES} (based on projected and measured SLOPE _{ASC} values) and a "transient" curve-fit scheme, smoothed sunspot numbers are projected for cycle 21 and compared to observed values. This approach is adequate to describe the gross behavior of smoothed sunspot number for cycle 21. Following the same approach, values of smoothed sunspot number are projected for cycle 22. An abbreviated version [21] of this report is to be published in the Proceedings of the Solar Terrestrial Prediction Workshop (18-22 June 1984, Moudon, France, P. A. Simon, Workshop Coordinator).					
17. Key Words (suggested by Author(s)) Sun, Sunspot Cycle, Sunspot Cycle Prediction, Solar Cycle			18. Distribution Statement  Unclassified - Unlimited		
19. Security Classif. (of this report) Unclassified		20. Security Classif. (of this page) Unclassified		21. No. of Pages 25	22. Price NTIS

ACKNOWLEDGMENTS

This work was suggested by Mr. Jesse B. Smith, Jr. (NOAA) who urged that a summary of our investigations into sunspot cycles be made available to Workshop attendees. Also, we are grateful to Dr. Ernest Hildner (NASA/MSFC) for critically reading the manuscript and to Drs. Ronald Moore and Steven Suess (NASA/MSFC) for helpful comments. We are especially grateful to Dr. Einar Tandberg-Hanssen (NASA/MSFC) who, in our absence, presented this paper (No. A.1.8, Long Term Solar Prediction) at the Solar Terrestrial Prediction Workshop.

TABLE OF CONTENTS

	Page
I. INTRODUCTION	1
II. APPROACH.....	1
III. RESULTS AND DISCUSSION	2
A. Sunspot Cycle Statistics	2
B. \bar{R}_{MAX} Versus SCN, An Empirical Curve-Fit.....	3
C. Linear Regression Equations Based on \bar{R}_{MAX}	6
D. Inferred Bi-Modal Distribution of Sunspot Cycles Based on Cycle Duration	8
E. A Transient Curve-Fit Scheme	10
F. Application of Empirical Method	11
IV. CONCLUSIONS	17
REFERENCES	18

LIST OF ILLUSTRATIONS

Figure	Title	Page
1.	Linear regression fit of the variation of \bar{R}_{MAX} versus SCN for modern sunspot cycles.....	4
2.	Empirical fit using a 3-component sinusoidal function (\bar{R}_{MAX} versus SCN).....	6
3.	Linear regression fits of $SLOPE_{ASC}$, \bar{R}_{MEAN} , and \bar{R}_{MIN} against \bar{R}_{MAX}	7
4.	Linear regression fits of MIN-MIN PERIOD, DES, and ASC against \bar{R}_{MAX}	7
5.	Linear regression fit of $SLOPE_{DES}$ against $SLOPE_{ASC}$	7
6.	Superposed epoch analysis curves for short-period and long-period cycles.....	9
7.	Variation of MIN-MIN PERIOD versus SCN	10
8.	Variation of transient-fit functional shape with value of m	11
9.	Comparison of observed and predicted smoothed sunspot numbers for SCN 21 using $SLOPE_{ASC}$ and $SLOPE_{DES}$	13
10.	Comparison of observed and predicted smoothed sunspot numbers for SCN 21 using the transient-fit scheme for two selected cases.....	14
11.	Prediction for SCN 22 using the $SLOPE_{ASC}$ and $SLOPE_{DES}$ fit and transient fit	16

LIST OF TABLES

Table	Title	Page
1.	Summary of Sunspot Cycle Information for the Modern Cycles.....	3
2.	Phase Information for the 3-Component Sinusoidal Fit	5
3.	Distribution of Cycle Duration	8
4.	Statistical Properties of Short-Period and Long-Period Sunspot Cycles	8

TECHNICAL MEMORANDUM

ESTIMATING SUNSPOT NUMBER

I. INTRODUCTION

The cyclic nature of sunspots has been a recognized solar phenomenon since about 1850, following the introduction by Rudolf Wolf in 1848 of the now well-known "relative sunspot number R " and the announcement by Heinrich Schwabe in 1843 of an apparent 10-year periodicity in sunspot observations made between 1826 and 1843. Until very recently, sunspot number had been routinely and systematically measured, following Wolf's numerical method, by the Swiss Federal Observatory in Zurich, Switzerland and its two branch stations in Arosa and Locarno; it was denoted R_Z . Beginning in January 1981, an "international" sunspot number, denoted R_I , has been measured by the Sunspot Index Data Center in Brussels, Belgium and replaced R_Z . The highest quality sunspot number data are regarded to be those which have been reported since about 1850 (Eddy [1]). Consequently, sunspot cycles dating back to Schwabe's original sunspot cycle, denoted sunspot cycle number (SCN) 8, are considered to be the most reliable and, thus, form the basis for a determination of statistical properties of sunspot cycles and for estimating the variation of sunspot number with time. The last completed cycle is SCN 20 which began in October 1964, peaked in November 1968, and ended in June 1976. SCN 21 began in June 1976, peaked in December 1979, and is now in decline. SCN 22, the next cycle, is expected to begin in the late 1980's (either late 1986 to early 1987 or late 1987 to early 1988, dependent upon cycle 21 being a short-period or long-period cycle, respectively; see Section III.D).

On the basis of smoothed sunspot number, denoted \bar{R}_{13} (also called "monthly moving average," "13-month running mean," etc.), for cycles 8 through 20, the following are examined: (1) sunspot cycle statistics, (2) an empirical curve-fit for R_{MAX} versus SCN where R_{MAX} is the maximum \bar{R}_{13} value for a cycle marking cycle maximum, (3) linear regression equations based on \bar{R}_{MAX} , (4) the inferred bi-modal distribution of sunspot cycles based on cycle duration, (5) a transient curve-fit scheme, and (6) application of these techniques to cycles 21 and 22. Section II describes the data base upon which this study is founded. Section III discusses the above topics in the stated order, and Section IV gives the conclusions. Much of this work has been extracted from previous studies which have been published elsewhere (e.g., Teuber, et al. [2,3] and Wilson [4,5,6]).

II. APPROACH

The Wolf relative sunspot number R is defined as

$$R = k(10^g + f) \quad , \quad (1)$$

where f is the total number of sunspots observed regardless of size, g is the number of observed sunspot groups, and k is a normalization parameter which varies from observatory to observatory to bring counts into agreement by accounting for telescope size, atmospheric opacity, etc. Sunspot counts are made daily and then averaged at the end of the month to obtain a monthly mean sunspot number. As stated in the introduction, monthly mean sunspot numbers of historical importance are those made and collated by the Swiss Federal Observatory located in Zurich, Switzerland, denoted R_Z . Waldmeier [7] has compiled values of R_Z for the period 1610 to 1960. Values of R_Z (now R_I) for the years since 1960 (actually, since 1944) are published monthly in Solar Geophysical Data—Prompt Reports (NOAA/Environment Research Laboratory, Boulder, Colorado USA).

For statistical comparisons, a smoothed sunspot number \bar{R}_{13} (also denoted \bar{R}_0 in Waldmeier [7]) has come into use. It is defined as

$$\bar{R}_{13} = \frac{R_{+6} + R_{-6} + 2 \sum_{i=-5}^{+5} R_i}{24}, \quad (2)$$

where R_{+6} is the monthly mean sunspot number 6 months ahead of the month of interest, R_{-6} is the monthly mean sunspot number 6 months behind the month of

interest, and $\sum_{i=-5}^{+5} R_i$ is the sum of the monthly mean sunspot numbers 5 months

either side and including the month of interest. In this study, use is made of smoothed sunspot number. Wilson [5] has compiled values of R_Z and \bar{R}_{13} for cycles 8 through 20 and part of cycle 21.

III. RESULTS AND DISCUSSION

A. Sunspot Cycle Statistics

Table 1 summarizes specific cycle-related parameters for cycles 8 through 20. It also gives parametric mean values and standard deviations for this group of cycles, and values for the parameters for cycle 21 when they are known. On the left, each cycle is identified by its sunspot cycle number (SCN). Adjacent to this and moving to the right are the parameters of interest: (1) the cycle minimum occurrence date (in month and year), (2) the cycle maximum occurrence date (in month and year), (3) \bar{R}_{MIN} (i.e., the \bar{R}_{13} value at cycle minimum occurrence), (4) \bar{R}_{MAX} (i.e., the \bar{R}_{13} value at cycle maximum occurrence), (5) ASC (i.e., the ascent period or time in months from cycle minimum occurrence to cycle maximum occurrence), (6) DES (i.e., the descent period or time in months from cycle maximum occurrence to subsequent cycle minimum occurrence), (7) MIN-MIN PERIOD (i.e., the cycle duration or time in months from cycle minimum occurrence to subsequent cycle minimum occurrence,

TABLE 1. SUMMARY OF SUNSPOT CYCLE INFORMATION FOR
THE MODERN CYCLES

SUNSPOT CYCLE NUMBER (SCN)	CYCLE MINIMUM	CYCLE MAXIMUM	\bar{R}_{MIN}	\bar{R}_{MAX}	ASC	DES	MIN-MIN PERIOD	\bar{R}_{MEAN}	SLOPE _{ASC}	SLOPE _{DES}
8	NOV 1833	MAR 1837	7.3	146.9	40	76	116	66.9	3.480	-1.795
9	JUL 1843	FEB 1848	10.5	152.0	55	94	149	55.9	2.209	-1.370
10	DEC 1855	FEB 1860	3.2	97.9	50	85	135	46.2	1.834	-1.091
11	MAR 1867	AUG 1870	5.2	140.5	41	100	141	52.9	3.300	-1.383
12	DEC 1878	DEC 1883	2.2	74.6	60	74	134	33.8	1.207	-0.941
13	FEB 1890	JAN 1894	5.0	87.9	47	96	143	38.5	1.764	-0.888
14	JAN 1902	FEB 1906	2.7	64.2	49	89	138	32.1	1.255	-0.704
15	JUL 1913	AUG 1917	1.5	105.4	49	71	120	44.0	2.120	-1.406
16	JUL 1923	APR 1928	5.6	78.1	57	65	122	40.3	1.272	-1.148
17	SEP 1933	APR 1937	3.5	119.2	43	82	125	57.2	2.651	-1.360
18	FEB 1944	MAY 1947	7.7	151.8	39	83	122	74.0	3.695	-1.788
19	APR 1954	MAR 1958	3.4	201.3	47	79	126	90.5	4.211	-2.427
20	OCT 1964	NOV 1968	9.6	110.6	49	91	140	59.9	2.061	-1.081
21	JUN 1976	DEC 1979	12.2	164.5	42	-	-	-	3.626	-
MEAN VALUES (CYCLES 8-20)			5.2	116.2	48.1	83.5	131.6	53.4	2.398	-1.337
STANDARD DEVIATIONS (CYCLES 8-20)			2.7	36.7	6.2	10.0	10.0	16.2	0.958	0.441

numerically equal to ASC + DES), (8) \bar{R}_{MEAN} (i.e., the mean \bar{R}_{13} value calculated over the entire cycle), (9) SLOPE_{ASC} [i.e., the line slope on the ascent side from \bar{R}_{MIN} to \bar{R}_{MAX} , computed as $SLOPE_{ASC} = [\bar{R}_{MAX}(SCN) - \bar{R}_{MIN}(SCN)] / ASC(SCN)$], and (10) SLOPE_{DES} [i.e., the line slope on the descent side from \bar{R}_{MAX} to subsequent cycle \bar{R}_{MIN} , computed as $SLOPE_{DES} = [\bar{R}_{MIN}(SCN + 1) - \bar{R}_{MAX}(SCN)] / DES(SCN)$]. Clearly, sunspot cycles, on average, range in smoothed sunspot number from about 5.2 ± 2.7 (i.e., mean value ± 1 standard deviation unit) at \bar{R}_{MIN} to about 116.2 ± 36.7 at \bar{R}_{MAX} and have a cycle duration of about 132 ± 10 months, with the descent period being about 1.8 times longer than the ascent period. A superposed-epoch analysis, based on mean \bar{R}_{13} values computed as a function of time t from \bar{R}_{MIN} occurrence for cycles 8 through 20, yields parametric values close to those summarized in Table 1. One minor difference is that \bar{R}_{MAX} is slightly reduced to about 106.9 ± 36.0 . In terms of range, from the lowest observed parametric value to the highest observed value for cycles 8 through 20, it is seen that \bar{R}_{MIN} has varied from 1.5 to 10.5, \bar{R}_{MAX} from 64.2 to 201.3, ASC from 39 to 60, DES from 65 to 100, and MIN-MIN PERIOD from 116 to 149.

B. \bar{R}_{MAX} Versus SCN, An Empirical Curve-Fit

In Figure 1, observed \bar{R}_{MAX} values are plotted against their respective SCN. For cycles 8 through 14, a downward trend is suggested, while an upward trend is suggested for cycles 14 through 20. For the whole set — i.e., cycles 8 through 20 — a time series regression reveals an upward trend, with \bar{R}_{MAX} being correlated positively with SCN approximately as

$$\bar{R}_{MAX} = 90 + 2 \text{ SCN} \quad .$$

ORIGINAL PAGE 19
OF POOR QUALITY.

(3)

The Pearson correlation coefficient r approximately equals 0.2 and the standard error of estimate S_{yx} , corrected for small sample size, is about 40.

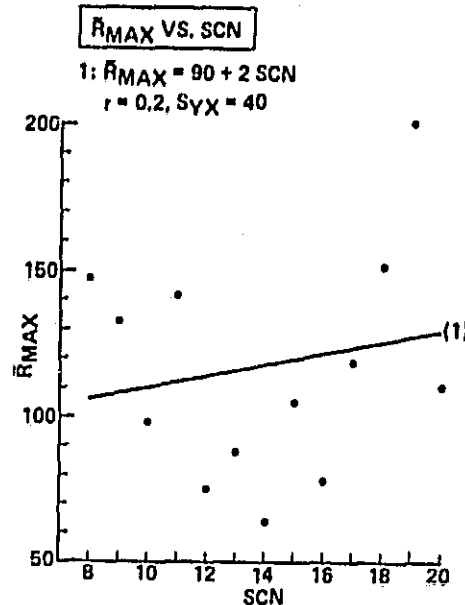


Figure 1. Linear regression fit of the variation of \bar{R}_{MAX} versus SCN for modern sunspot cycles.

Eddy [1,8-10] has done considerable research on the historical record of sunspot data and solar activity. His studies, based primarily on naked-eye and early telescopic sunspot observations, fossil radiocarbon levels in tree rings, and auroral reports, have suggested possibly strong climatic associations in the Sun-Earth record; in particular, he has found evidence for the occurrence of prolonged "sunspot minima" (e.g., the Spörer Minimum — A.D. 1400-1510, and the Maunder Minimum — A.D. 1645-1715) and a prolonged "sunspot maximum" (the so-called Medieval Maximum or Grand Maximum — ca., A.D. 1120-1280). If it is assumed that such sunspot minima and maximum have indeed happened and that they reflect periods when sunspot number was relatively lower and higher, respectively, equation (3) can be approximated by equation (4), given below as

$$\bar{R}_{MAX} = 120 + 25 \sin \theta_1(x) \quad . \quad (4)$$

Equation (4) is of the form $y = a_0 + a_1 \sin \theta_1(x)$, where y is \bar{R}_{MAX} , as before, and $\theta_1(x)$ is the phase of an SCN, within a 90-cycle periodicity. The coefficient a_0 was selected to have a value approximately equal to the value given by equation (3) for SCN 14, the midpoint of the modern data set. The coefficient a_1 represents a "best-fit" (to the sum of the squares of the residuals) for the given a_0 and values of $\theta_1(x)$

contained in Table 2. The 90-cycle periodicity of \bar{R}_{MAX} , which is used to approximate the linear regression equation [equation (3)], is based on Eddy's suggestion that a Grand Maximum really existed, having a peak value at SCN ≈ -53 , and that the Maunder Minimum likewise existed. The time difference between Grand Maximum and Maunder Minimum is about 500 years or 45 sunspot cycles, of 11 years average duration; hence, the period of 90 cycles results. At SCN ≈ -53 , $\theta_1(x) = 90$ degrees is defined so that \bar{R}_{MAX} is at maximum value. The 90-cycle periodicity causes each cycle to increment by 4 degrees; thus, for cycles 8 through 20, $\theta_1(x)$ varies between 334 and 22 degrees, respectively. (See Wilson [6] for additional comments.)

TABLE 2. PHASE INFORMATION FOR THE 3-COMPONENT SINUSOIDAL FIT

X-VARIABLE	90-CYCLE	11-CYCLE	2-CYCLE		
SCN	$\theta_1(x)$	$\theta_2(x)$	$\theta_3(x)$	$\bar{R}_{MAX}(\text{COMP})^1$	$\bar{R}_{MAX}(\text{OBS})$
8	334	90.0	270	129.0	146.9
9	338	122.7	90	155.1	132.0
10	342	155.5	270	118.8	97.9
11	346	188.2	90	124.0	140.5
12	350	220.9	270	77.7	74.6
13	354	253.6	90	98.8	87.9
14	358	286.4	270	70.6	64.2
15	2	319.1	90	113.0	105.4
16	6	351.8	270	102.6	78.1
17	10	24.5	90	153.9	119.2
18	14	57.3	270	140.5	151.8
19	18	90.0	90	177.7	201.3
20	22	122.7	270	143.8	110.6
21	26	155.5	90	(160.5)	164.5
22	30	188.2	270	(112.5)	--

$$^1 \bar{R}_{MAX}(\text{COMP}) = 120 + 26 \sin \theta_1(x) + 36 \sin \theta_2(x) + 15 \sin \theta_3(x) \quad (\text{EQ. (5)})$$

$$\text{RES} = \bar{R}_{MAX}(\text{COMP}) - \bar{R}_{MAX}(\text{OBS})$$

$$\sum (\text{RES})^2 = 5137.9 - \text{VARIANCE} = \frac{\sum (\text{RES})^2}{N} = \frac{5137.9}{13} = 395.2 = S^2$$

$$S = 19.9$$

$$\text{VARIANCE OF MEAN} = 1543.9 - \text{EQ. 5 REDUCES VARIANCE BY 70\%}$$

Returning to Figure 1, it is reiterated that there is an apparent downward trend in \bar{R}_{MAX} values for SCN 8 through 14 and an upward trend for SCN 14 through 20.

Closer inspection reveals that, in addition to this variation, there is an "up-down-up" signature, especially between SCN 10 and 17. Together, these two observations suggest that the \bar{R}_{MAX} versus SCN plot might be better fitted using a 3-component sinusoidal curve, one component being a 90-cycle periodicity, mentioned above, a second component being an 11-cycle periodicity, and a third component being a 2-cycle periodicity. Such an analysis yields the relation

$$\bar{R}_{MAX} = 120 + 25 \sin \theta_1(x) + 35 \sin \theta_2(x) + 15 \sin \theta_3(x) \quad , \quad (5)$$

where values for $\theta_1(x)$, $\theta_2(x)$, and $\theta_3(x)$ are contained in Table 2. It is seen, then, that for any modern SCN, an approximate value for \bar{R}_{MAX} can be deduced, which is based on a fit that has a smaller variance than that for the mean. As compared to the mean, the total variance using equation (5) has been reduced by about 70 per cent; thereby, achieving a standard deviation s of about 20.

Figure 2 compares computed and observed values of \bar{R}_{MAX} for cycles 8 through 21, where the computed \bar{R}_{MAX} values are calculated using equation (5). The two curves behave similarly and all of the observed \bar{R}_{MAX} values lie within 1.5 s units (i.e., ± 30) of the computed \bar{R}_{MAX} values. It should be emphasized that the fit is based strictly on a fit of SCN 8 through 20, and, as such, it may be of little or no predictive value for future cycles. Its worth becomes apparent only after it has successfully predicted several successive cycles. It is noted, however, that equation (5) predicts SCN 21 to have an \bar{R}_{MAX} value of about 160, which is remarkably close to its observed \bar{R}_{MAX} value, now known to have been about 165, a prediction accurate to within a few percent.

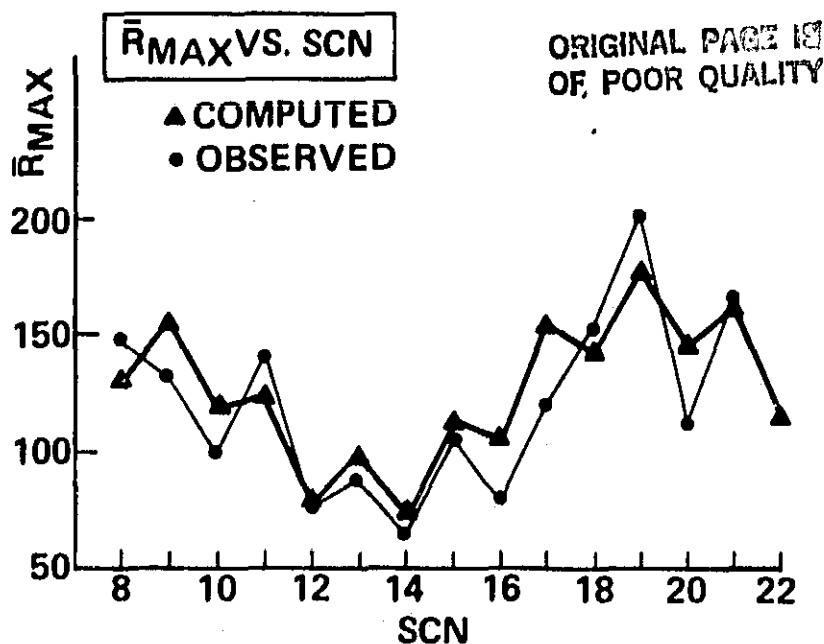


Figure 2. Empirical fit using a 3-component sinusoidal function (\bar{R}_{MAX} versus SCN).

C. Linear Regression Equations Based on \bar{R}_{MAX}

Now that a reasonable estimate for \bar{R}_{MAX} is possible, from equation (5), other cycle-related parameters can be estimated using results of linear regression analysis,

based on observed values of \bar{R}_{MAX} as the independent variable (Wilson [5,6]). Figures 3 and 4 depict regression equations for the parameters listed in Table 1, based on a comparison to \bar{R}_{MAX} . Figure 3 illustrates the variation of $SLOPE_{ASC}$, \bar{R}_{MEAN} , and \bar{R}_{MIN} with \bar{R}_{MAX} . Both $SLOPE_{ASC}$ and \bar{R}_{MEAN} show strong "positive" correlation, having a Pearson correlation coefficient r greater than 0.9. On the other hand, \bar{R}_{MIN} , although correlated in a positive sense with \bar{R}_{MAX} , has an r of only about 0.3, indicating that the correlation is, at best, weak. Figure 4 plots MIN-MIN PERIOD, DES, and ASC against \bar{R}_{MAX} . ASC shows the strongest correlation of these three parameters, being negatively correlated with \bar{R}_{MAX} and having an r of about -0.6. The rather strong correlations of $SLOPE_{ASC}$ and ASC with \bar{R}_{MAX} , while not independent, amply confirm that cycles with high maximum sunspot numbers get their maxima more swiftly, rather than by sustaining their growth rates longer than cycles with lower maxima. Figure 5 plots $SLOPE_{DES}$ against $SLOPE_{ASC}$ and shows the strong negative correlation ($r \approx -0.9$) expected from the earlier, individual regressions against \bar{R}_{MAX} .

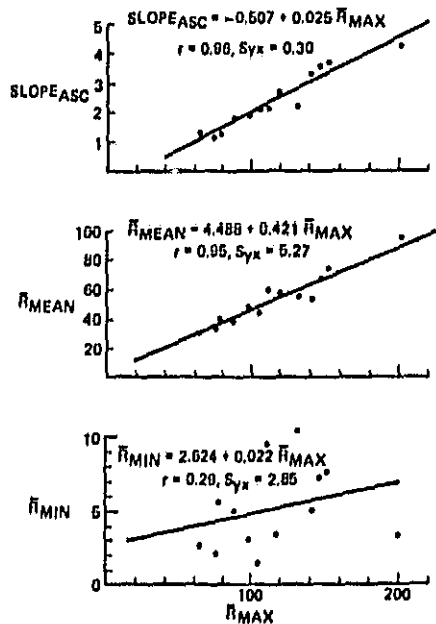


Figure 3. Linear regression fits of $SLOPE_{ASC}$, \bar{R}_{MEAN} , and \bar{R}_{MIN} against \bar{R}_{MAX} .

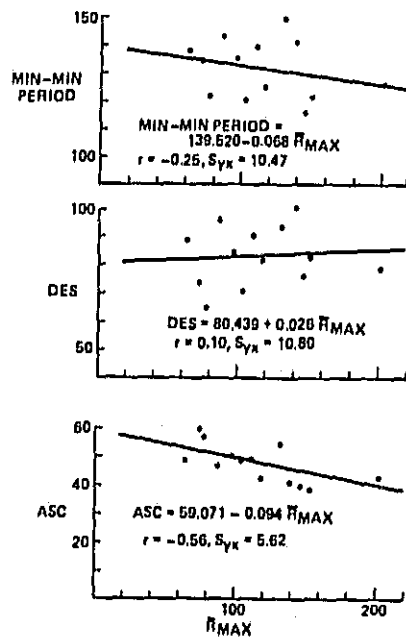


Figure 4. Linear regression fits of MIN-MIN PERIOD, DES, and ASC against \bar{R}_{MAX} .

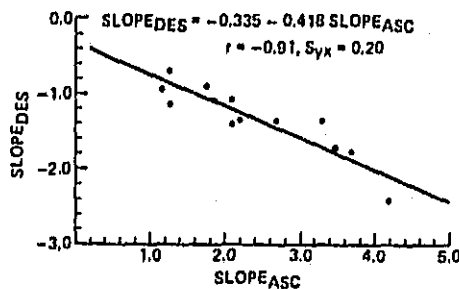


Figure 5. Linear regression fit of $SLOPE_{DES}$ against $SLOPE_{ASC}$.

D. Inferred Bi-Modal Distribution of Sunspot Cycles
Based on Cycle Duration

From Table 1, it is discerned that, although sunspot cycles average about 132 months in duration, there have been no sunspot cycles in the entire set of SCN 8 through 20 which have a cycle duration in the range 127 to 133 months. All cycles have either a minimum-to-minimum period shorter than 127 months or longer than 133 months (Wilson [5] and Wilson et al. [11]). This bifurcation of cycle duration is readily seen in Table 3. Cycles 8 and 15 through 19 have cycle duration between 116 and 126 months and cycles 9 through 14 and 20 have cycle duration between 134 and 149 months. Excluding cycle 9 which has the longest cycle duration on record, being 149 months, the range is between 134 and 143 months. Thus, sunspot cycles appear to be distributed by cycle duration into two distinct groupings: (1) a short-period cycle group, having a mean period of about 122 months with a standard deviation of about 3 months, and (2) a long-period cycle group, having a mean equal to about 140 months and a standard deviation equal to about 5 months; excluding SCN 9 reduces the mean for the long-period cycle group to 138.5 with a standard deviation of 3.2. A summary is provided in Table 4.

TABLE 3. DISTRIBUTION OF CYCLE DURATION

CYCLE DURATION INTERVAL (MONTHS)	FREQUENCY OF OCCURRENCE	SCN'S
116 - 121	2	8*, 15
122 - 127	4	16, 17, 18, 19
128 - 133	0	
134 - 139	3	10, 12, 14
140 - 145	3	11, 13, 20
146 - 151	1	9**

*SUNSPOT CYCLE 8 HAS THE SMALLEST CYCLE DURATION EQUAL TO 116 MONTHS

**SUNSPOT CYCLE 9 HAS THE LARGEST CYCLE DURATION EQUAL TO 149 MONTHS

NOTE: NO CYCLE DURATION HAS BEEN REPORTED WITH A VALUE BETWEEN 127 AND 133.

TABLE 4. STATISTICAL PROPERTIES OF SHORT-PERIOD AND LONG-PERIOD SUNSPOT CYCLES

CYCLE GROUP	SCN'S	MEAN CYCLE DURATION	STANDARD DEVIATION	RANGE
SHORT-PERIOD	8, 15-19	121.8	3.3	116-126
LONG-PERIOD: (1)	9-14, 20	140.0	4.7	134-149
	(2)* 10-14, 20	138.5	3.2	134-143
ALL	8 - 20	131.6	10.0	116-149

*EXCLUDES SCN 9

A superposed-epoch analysis for each of these two cycle groupings results in the curves depicted in Figure 6. It is seen that short-period cycles are characterized as cycles which reach maximum more quickly and have a higher \bar{R}_{MAX} than long-period cycles. For short-period cycles, \bar{R}_{MAX} averages about 127 with a standard deviation of about 41 (at maximum), reaching maximum in about 44 months. On the other hand, long-period cycles average about 92 at \bar{R}_{MAX} with a standard deviation of about 22, reaching maximum in about 50 months.

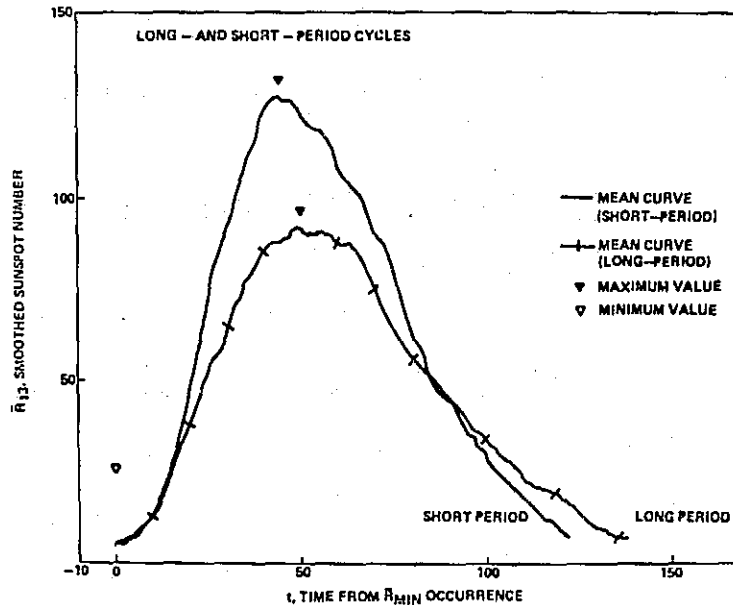


Figure 6. Superposed epoch analysis curves for short-period and long-period cycles.

Returning to Table 1, it is observed that of the six cycles that had cycle duration less than the average cycle duration (i.e., the short-period cycles), four had an \bar{R}_{MAX} value which exceeded the average \bar{R}_{MAX} value. Also, of the cycles with $\bar{R}_{MAX} \geq 142$, all (3 of 3) have been short-period cycles. Of the seven cycles catalogued as long-period cycles, five had an \bar{R}_{MAX} value lower than average. Thus, 9 of 13 sunspot cycles fit the pattern where short-period cycles are associated with high-valued \bar{R}_{MAX} cycles and long-period cycles with low-valued \bar{R}_{MAX} cycles. Therefore, a "crude" means is reached whereby cycle duration can be estimated on the basis of \bar{R}_{MAX} .

While a plot of \bar{R}_{MAX} versus SCN (Figs. 1 and 2) shows a downward trend followed by an upward trend, being centered at about SCN 14, it is seen that a plot of minimum-to-minimum period versus SCN (Fig. 7) gives the appearance of a "square wave," albeit there are really too few sunspot cycles to make a bona fide assessment. (See Wilson, et al. [11] concerning the behavior of cycle duration with time.) Placement of cycle 21 on the plot is, thus, seen to be largely conjectural, being either about 140 if the "square-wave" pattern is legitimate, suggesting that cycle 21 is a long-period cycle, or being about 122 if the association between short-period cycles and high-valued \bar{R}_{MAX} cycles is the stronger. If the latter is true, then, either the "square-wave" pattern is merely illusory or cycle 20 may have been anomalous (see Section III.F).

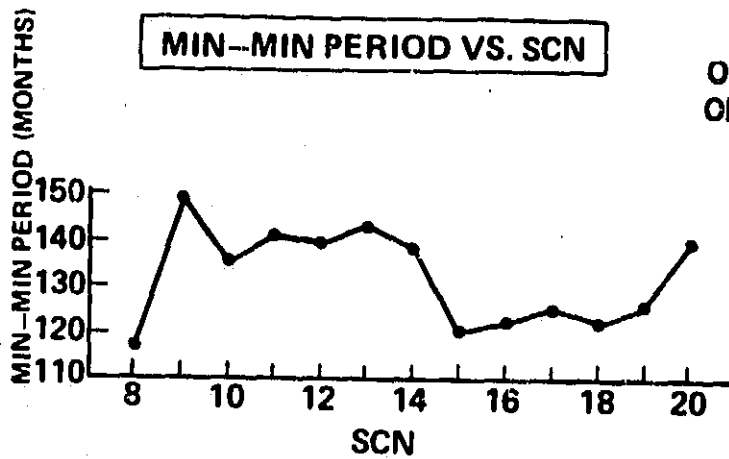


Figure 7. Variation of MIN-MIN PERIOD versus SCN.

E. A Transient Curve-Fit Scheme

In an earlier paper, Teuber, et al. [2] developed an analytical method for fitting impulsive transient phenomena; in particular, for light curves of X-ray flares. A formula was derived, given as

$$Y = A (Bt)^m e^{-Bt} + Y_0 \quad , \quad (6)$$

where Y is the magnitude of the pulse calculated for a particular t, the time from the start of the pulse, and Y₀ is an offset or background reference (calculated at t = 0). A and B are constants, A being the pulse height and B being the pulse width. Values for A and B are computed as

$$A = (Y_M - Y_0) m^{-m} e^m \quad (7)$$

and

$$B = m (ASC)^{-1} \quad , \quad (8)$$

where Y_M is the maximum magnitude of the pulse, ASC the ascent period of the pulse, and m an exponent which had the value of 3/2 in the X-ray flare study.

Sunspot cycles, perhaps, show an analogous transient behavior and may be fitted with equations of the form of equations (6), (7), and (8). Now, Y_M corresponds to the maximum smoothed sunspot number at cycle maximum (\bar{R}_{MAX}), Y₀ the minimum smoothed sunspot number at cycle minimum (\bar{R}_{MIN}), ASC the ascent period of the cycle, and t the time in months from cycle minimum. Once these parameters are set, m can be varied to determine the best fit. (In practice, one would allow Y_M, Y₀, ASC, and m to vary to achieve the best fit.)

Figure 8 illustrates the effect of varying m . A high value of m means that the curve initially begins to change more slowly than lower values of m , but rises more steeply as t approaches ASC. Furthermore, a high value of m means that the curve falls off more steeply than lower values of m just after peak, but more slowly as $t \gg$ ASC. A fit of the superposed-epoch analysis curves, shown in Figure 6, suggests that m has a value of about 3.8 on the ascent side and 4.3 on the descent side for short-period cycles, and a value of 3.6 and 3.8 on the ascent and descent sides, respectively, for long-period cycles. Thus, using equation (5) to determine an initial estimate for R_{MAX} and then, assuming that the cycle in question is either a long-period or short-period cycle, equations (6), (7), and (8) can be applied to determine intermediate values of R_{13} during the cycle. This initial sunspot cycle curve prediction can then be adjusted to better fit observed R_{13} values as they become known. (Wilson [5] has found additional ways to deduce R_{MAX} once the cycle has started. These other means are based on the magnitude of the rate of change of smoothed sunspot number during its ascent and on the magnitude of the sum of monthly mean sunspot numbers, prior to $t = 24$ months. Both are found to correlate well with R_{MAX} .)

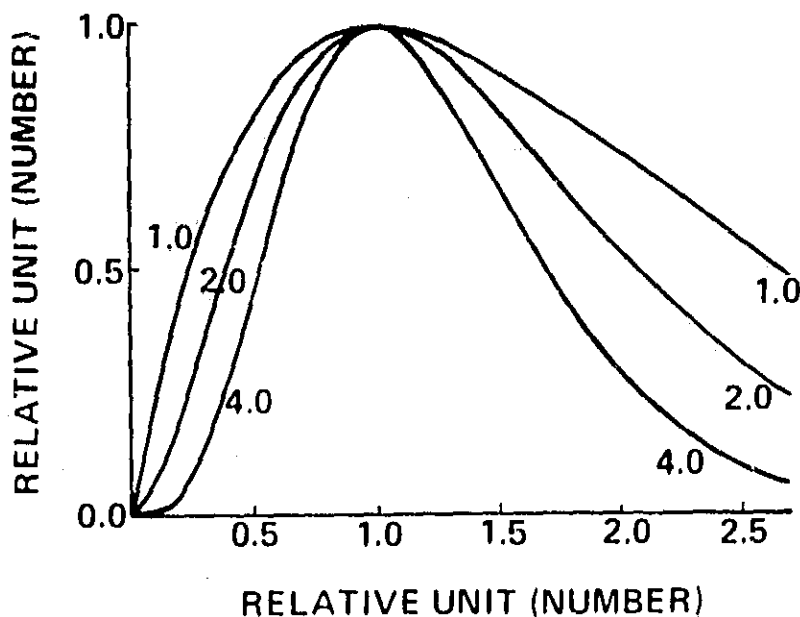


Figure 8. Variation of transient-fit functional shape with value of m .

F. Application of Empirical Method

1.0 Cycle 21

Having laid a foundation for estimating sunspot number as a function of time from cycle minimum, based on the behavior of cycles 8 through 20, the technique is now applied to cycles 21 and 22. The goal, of course, is to more accurately describe these cycles and their cycle-related parameters than can be achieved by using mean cycle statistics.

Based on mean cycle statistics, cycle 21 would be expected to have an \bar{R}_{MAX} value of approximately 116.2 ± 36.7 (i.e., the mean value ± 1 unit of standard deviation accuracy), or 106.9 ± 36.0 if the superposed-epoch analysis curve is used for the mean sunspot cycle. It should reach maximum in about 48 ± 6 months, decay to subsequent cycle minimum in about 84 ± 10 months, thus having a cycle duration of about 132 ± 10 months, and have an \bar{R}_{MEAN} of about 53 ± 16 . If cycle 21 is regarded to be a short-period cycle, its \bar{R}_{MAX} should be about 127.1 ± 41.4 , its ASC equal to about 44 months, and its DES equal to about 78 months, yielding a cycle duration of about 122 ± 3 months. Certainly, it would be expected to lie within or very near the range of previously observed short-period cycles which is 116 to 126 months. On the other hand, if cycle 21 is a long-period cycle, then its \bar{R}_{MAX} should be about 91.8 ± 22.0 , its ASC equal to about 50 months, and its DES equal to about 90 months, yielding a cycle duration of about 140 ± 5 months. As a long-period cycle, it would be expected to have a cycle duration within or very near the range of previously observed long-period cycles which is 134 to 149 months (excluding SCN 9, 13/4 to 143 months).

Application of equation (5), using the $\theta_1(x)$, $\theta_2(x)$, and $\theta_3(x)$ values contained in Table 2, as shown in Figure 2, predicts that cycle 21 should have an \bar{R}_{MAX} of about 160 ± 20 . This is remarkably close to the value of 154 predicted for cycle 21 by Sargent [13] and to the actually observed value of 164.5. Using the linear regression equations identified in Figures 3, 4, and 5, which are based on comparisons to observed values of \bar{R}_{MAX} , a $SLOPE_{ASC}$ of about 3.5 ± 0.3 , a $SLOPE_{DES}$ of about -1.8 ± 0.2 , and an \bar{R}_{MEAN} of about 71.8 ± 5.3 can be projected for cycle 21. $SLOPE_{ASC}$ for cycle 21 has now been observed and its value is 3.63, very close to that predicted from the linear regression equation. Using the observed $SLOPE_{ASC}$ value, $SLOPE_{DES}$ for cycle 21 is redetermined to be -1.85.

ASC for cycle 21 is now known to be 42 months, very close to that expected for short-period cycles, and significantly different from the value expected for long-period cycles. Likewise, it is now known that \bar{R}_{MAX} for cycle 21 is 164.5, making it a high-valued \bar{R}_{MAX} cycle, the second highest in the set SCN 8 through 21. It may be surmised, then, that cycle 21 is very probably a short-period cycle. Thus, it is expected to have a cycle duration of about 122 ± 3 months, implying that $DES = 80 \pm 3$ months. This means that \bar{R}_{MIN} for cycle 22 may occur as early as August 1986 ± 3 months, much earlier than the June 1987 date calculated from the average 11-year cycle duration, or later dates if SCN 21 is a long-period cycle. Yoshimura [14] has also suggested that cycle 21 will be a short-period cycle, as have Otaola and Zenteno [15]. Yoshimura bases his prediction on a repeating pattern of "grand cycles," each of 5-cycle duration; Otaola and Zenteno base their prediction on application of a non-integer technique of power spectral analysis. Note that if cycle 21 is indeed a short-period cycle, then its minimum-to-minimum period will not fit the supposed "square-wave" pattern depicted in Figure 7, implying, perhaps, that the pattern is merely coincidental or that cycle 20 may have been anomalous. When cycle 20 is compared to the most recent cycles, it certainly appears to have been anomalous, especially in terms of its \bar{R}_{MAX} value. (See Wilson, et al. [11] for additional comments concerning the behavior of cycle duration with time.) In this cited paper,

based on an investigation of "trends" in the sunspot record, a statistic is identified which strongly suggests that cycle 21 is a long-period cycle, with \bar{R}_{MIN} for cycle 22 occurring about February 1988, very close to that predicted by Holland and Vaughan [16], based on a Lagrangian least-squares fit of smoothed 2800 MHz radio flux. (See also Xu, et al. [17].)

In addition, it must be noted that Fairbridge and Hameed [18] have predicted cycle 22 minimum occurrence to be 1989.1 ± 0.9 , on the basis of a suggested repeating pattern of sunspot minima every 178 years; thereby, implying that cycle 21 is a long-period cycle of period equal to about 151 months, almost 4 standard deviation units longer than the mean for long-period cycles (excluding SCN 9). (See also Jose [19] and Gregg [20].) A period of 151 months implies that the descent period for cycle 21 will be 109 months, nearly 2.6 standard deviation units longer than the mean descent period for cycles 8 through 20. Together, this seems to suggest that cycle 21 is very improbably a long-period cycle, being much more likely a short-period cycle. The analysis of Fairbridge and Hameed, as that of Jose, Gregg and the other aforementioned analyses, is based, in part, on sunspot data prior to SCN 8. It is recalled that sunspot data prior to SCN 8 are not considered to be as reliable as that for cycles occurring after SCN 8. This may mean that the supposed association between sunspot minimum occurrences and the 178-year rhythm of the solar orbit around the center of mass of the solar system is not as strong as has been previously believed. (Note, however, that if the lower limit of the Fairbridge and Hameed result is used, namely that SCN 22 will begin about 1988.2, then this is consistent with SCN 21 being a long-period cycle with cycle minimum for SCN 22 occurring about February 1988.)

Figure 9 compares observed \bar{R}_{13} values with those predicted for cycle 21, based on the \bar{R}_{MAX} prediction of equation (5) and the observed \bar{R}_{MIN} value. Two $SLOPE_{ASC}$ and $SLOPE_{DES}$ lines are drawn. The heavy lines are associated with the observed $SLOPE_{ASC}$ value; the light lines are associated with the predicted $SLOPE_{ASC}$ value.

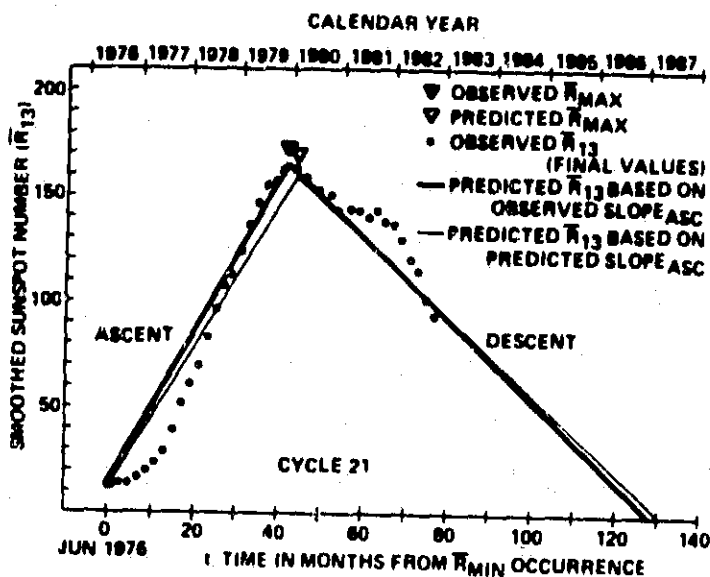


Figure 9. Comparison of observed and predicted smoothed sunspot numbers for SCN 21 using $SLOPE_{ASC}$ and $SLOPE_{DES}$.

ORIGINAL PAGE NO.
OF POOR QUALITY

The dots represent observed \bar{R}_{13} values. The figure shows that $\text{SLOPE}_{\text{ASC}}$, whether the predicted slope or the observed slope is used, fits the observed \bar{R}_{13} values reasonably well, especially for $t > 20$. Cycle 21 is observed to have had a period of about 6 months, just after \bar{R}_{MIN} occurrence, when \bar{R}_{13} remained essentially constant. At $t = 6$, observed \bar{R}_{13} values are seen to rise nearly linearly to \bar{R}_{MAX} occurrence, which was at $t = 42$. There has been one significant "bump" in the decline of cycle 21, reminiscent of the behavior of cycle 20 (which was a long-period cycle), occurring approximately 21 months after \bar{R}_{MAX} occurrence.

Figure 10 compares a fit, based on equations (6), (7), and (8), with the observed \bar{R}_{13} values for cycle 21. The comparison is made for two different epochs: (1) post- \bar{R}_{MIN} occurrence, but prior to \bar{R}_{MAX} occurrence and (2) post \bar{R}_{MIN} and \bar{R}_{MAX} occurrences. For the first case (Fig. 10, bottom), $\bar{R}_{\text{MIN}} = 12.2$ and \bar{R}_{MAX} is assumed to be 160, based on the prediction of equation (5). An m equal to 3.8 on the ascent side and 4.3 on the descent side is used; i.e., the mean m values for the

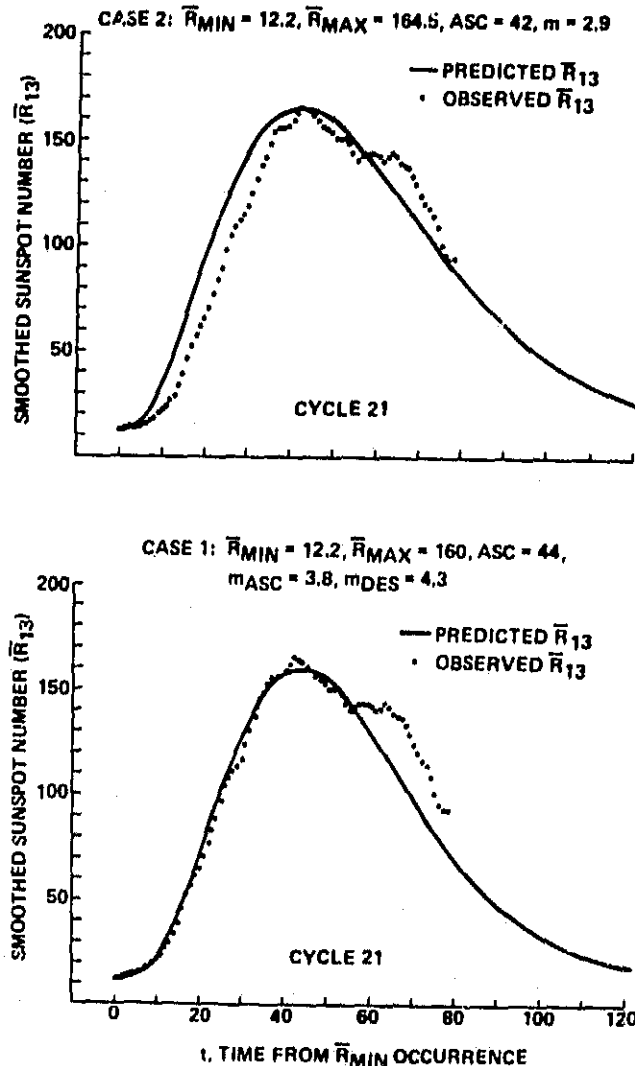


Figure 10. Comparison of observed and predicted smoothed sunspot numbers for SCN 21 using the transient-fit scheme for two selected cases.

short-period cycle group have been applied. An ASC of 44 months is employed. It is noted that there is very close agreement between observed and predicted values for $0 \leq t \leq 55$. For $t > 55$, corresponding to the "bump" in the decline of cycle 21, the curves are in disagreement. Observed values of \bar{R}_{13} have remained significantly higher than the plotted curve. It is as though the predicted decline curve has been shifted about six months to the right. The "bump" can also be approximated as the superposition of two "transient" pulses, with peaks separated by about 1.5 to 2 years, although such a fit is not shown here. This may be an indication that this cycle, like its predecessor cycle 20, may have one or more "bumps" during its decline and that these "bumps" may be the result of short-term periodicities in the sunspot cycle, shorter than the 11-year average cycle duration (see Wilson [5,6] and references contained therein).

For the second case (Fig. 10, top), $\bar{R}_{MIN} = 12.2$, $\bar{R}_{MAX} = 164.5$, $ASC = 42$, and $m = 2.9$ (the "best-fit" value of m for $0 \leq t \leq 78$; i.e., data through December 1982). The curve shown represents the "best-fit" using all data from June 1976 through December 1982, which includes the "bump." A "best-fit" for all data prior to the "bump," i.e., $0 \leq t \leq 55$, yields a value for m of about 5.0. Thus, the effect of the "bump" is to significantly lower the value of m during descent, at least for $t \leq 78$. If cycle 21 is a short-period cycle, the "best-fit" m value must increase in value for $t > 78$, which effectively lowers the predicted \bar{R}_{13} values. Otherwise, at $t = 122$, a time when \bar{R}_{13} should be at or very near \bar{R}_{MIN} , the predicted \bar{R}_{13} values will be too high. For $m = 5.0$, the standard deviation s about the predicted curve (not shown) for the ascent period $t \leq 42$, is about 5.4. For $m = 2.9$, the "best-fit" for $t \leq 78$ including the "bump," s is about 13.0.

2.0 Cycle 22

Cycle 22 begins when \bar{R}_{13} has reached a minimum value in the decline of cycle 21. As stated above, based on the statistics of cycles 8 through 20, cycle 21 is expected to be a short-period cycle; consequently, its minimum-to-minimum period should be about 122 ± 3 months. As a short-period cycle, cycle 21 would be expected to be less than 128 months and more than 116 months in duration. Hence, \bar{R}_{MIN} for cycle 22 should occur between February 1986 and February 1987, with the "best-guess" being about August 1986. If cycle 21 is a long-period cycle, as suggested by Figure 7, then \bar{R}_{MIN} for cycle 22 will occur about February 1988.

Application of equation (5), using the $\theta_1(x)$, $\theta_2(x)$, and $\theta_3(x)$ values for cycle 22 in Table 2, predicts that cycle 22 will have an \bar{R}_{MAX} value of about 110 ± 20 (Fig. 2), a value being about that observed for SCN 20. Using the linear regression equations identified in Figures 3, 4, and 5, which are based on comparisons to \bar{R}_{MAX} , we project $SLOPE_{ASC}$ to be about 2.2 ± 0.3 , $SLOPE_{DES} -1.3 \pm 0.2$, and $\bar{R}_{MEAN} 50.8 \pm 5.3$. A value of $\bar{R}_{MAX} = 110$ implies that cycle 22 will be a low-valued \bar{R}_{MAX} cycle; consequently, it is expected to be a long-period cycle. As a long-period cycle, it should have an ASC of about 50 months and a total cycle duration of about 140 months.

On the basis that cycle 22 will be a long-period cycle with $ASC = 50$ months, Figure 11 (bottom) plots the anticipated $SLOPE_{ASC}$ and $SLOPE_{DES}$ lines. This approach yielded quite reasonable values for cycle 21 (recall Fig. 9), so it is anticipated that it will yield reasonable values for \bar{R}_{13} here. Therefore, cycle 22 is predicted to reach a maximum of $\bar{R}_{MAX} = 110 \pm 20$ about October 1990 (± 6 months), and to reach subsequent cycle \bar{R}_{MIN} about April 1998. (These dates are based on cycle 21 being a short-period cycle. Other dates have been summarized in the abstract, on the basis of SCN 21 and 22 being either long-period or short-period cycles.) A projection for cycle 22 using the "transient" fit approach is also depicted in Figure 11 (top), where $\bar{R}_{MIN} = 5$, $\bar{R}_{MAX} = 110$, $ASC = 50$, and $m = 3.7$, the value for m midway between m_{ASC} and m_{DES} for long-period cycles. It is emphasized that Figure 11 presents the "best guess" for the general behavior of cycle 22. Until cycle 22 commencement has occurred, this prediction cannot be improved. Also, the technique in its present form does not allow the anticipation of the occurrence of "bumps" following \bar{R}_{MAX} occurrence, as has been seen for cycles 20 and 21.

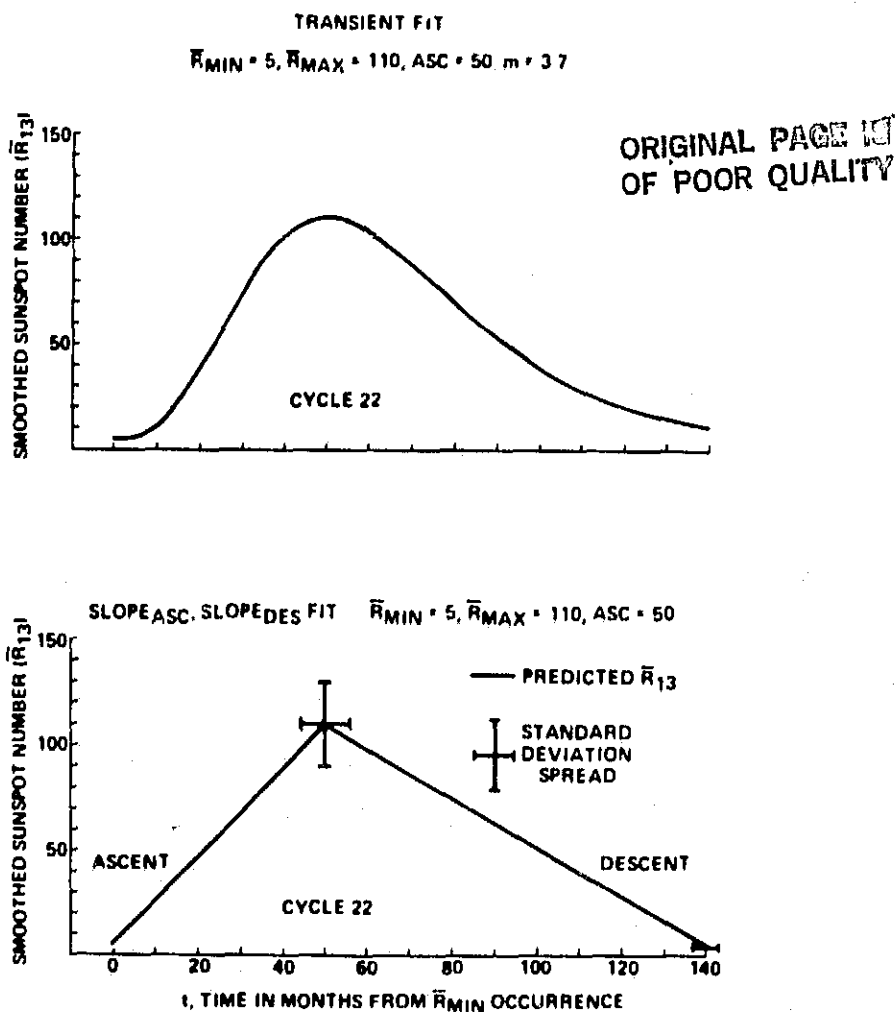


Figure 11. Prediction for SCN 22 using the $SLOPE_{ASC}$ and $SLOPE_{DES}$ fit and the transient fit.

Another estimation for cycle 22, on the basis of paired-cycle duration using principal component analysis, is that cycle 22 \bar{R}_{MAX} will be about 120 ± 30 (Teuber [12]). This is consistent with what has been predicted here, and also to that predicted by Holland and Vaughan [16] based on a Lagrangian least-squares prediction of smoothed 2800-MHz radio flux. They predict cycle 22 to have a peak smoothed 2800-MHz radio flux of about 150 which, based on a linear regression comparison given by Wilson [5], yields a peak smoothed sunspot number of about 95. Also, Xu, et al. [17] have predicted cycle 22 to have an \bar{R}_{MAX} between 90 and 106. It must be noted, however, that these predictions are in disagreement with that predicted by Gregg [20], based on a novel oscillator model; he predicts cycle 22 to begin in 1988, peak about 1994 with an annual mean sunspot number of about 36, and have a descent period shorter than its ascent period, reaching the following minimum in 1999. (Wilson [6] has shown that maximum annual values of sunspot number are very close in value to \bar{R}_{MAX} values; for a maximum annual value of 36, \bar{R}_{MAX} is expected to be about 39.) Negative skewness, that is ascent duration being longer than descent duration, is non-existent in the sunspot data for cycles 8 through 21. If one includes cycles 1 through 7, as has been done by Gregg, then there may have been at least a few examples of negative skewness. (We remind the reader that sunspot data for cycles prior to SCN 8 are considered to be unreliable.)

IV. CONCLUSIONS

In this study, a simple empirical method has been developed to predict certain parameters of future solar activity cycles — e.g., \bar{R}_{MAX} , ASC, DES, MIN-MIN PERIOD, \bar{R}_{MEAN} , $SLOPE_{ASC}$, and $SLOPE_{DES}$. The method is based on cycles 8 through 20 and incorporates a 3-component sinusoidal fit of \bar{R}_{MAX} values versus sunspot cycle number, where the three sinusoidal components include a 90-cycle, an 11-cycle, and a 2-cycle periodicity. (Linear regression equations, based on \bar{R}_{MAX} , allow for the evaluation of the aforementioned cycle-related parameters.) A "transient" curve-fit scheme is also presented which allows for a month-by-month prediction of smoothed sunspot number from \bar{R}_{MIN} occurrence for a given cycle. The empirical method has been applied to cycle 21, as an example, and found to work very well. Had it been used early in the cycle, it would have predicted an \bar{R}_{MAX} value of about 160 for cycle 21, compared to the actually observed \bar{R}_{MAX} value of 164.5. (If cycle 21 turns out to be a cycle of short duration (that is, a cycle having a duration of 122 ± 3 months) rather than a cycle of long duration (duration 140 ± 5 months), then cycle 22 should begin about August 1986, certainly before February 1987. An \bar{R}_{MAX} value of 110 ± 20 is projected for cycle 22, occurring about 50 months after \bar{R}_{MIN} occurrence, or about October 1990 (± 6 months). Cycle 22 is projected to be a cycle of long duration; hence, it should end about April 1998. If instead cycle 21 turns out to be a cycle of long duration, then cycle 22 will not begin until about February 1988, peak until about April 1992 and end until about October 1999.

REFERENCES

1. Eddy, J. A.: Historical Evidence for the Existence of the Solar Cycle. The Solar Output and Its Variation, edited by O. R. White, Colorado Associated University Press, Boulder, Colorado, 1977, pp. 51-71.
2. Teuber, D. L.; Reichmann, E. J.; Wilson, R. M.; and Smith, J. B., Jr.: A Prediction Method for the Soft X-Ray Flux of Solar Flares. Solar-Terrestrial Predictions Proceedings (Solar Activity Predictions), edited by R. F. Donnelly, Vol. III, Boulder, Colorado, 1980, pp. C173-C188.
3. Teuber, D. L.; Reichmann, E. J.; and Wilson, R. M.: Description of Sunspot Cycles by Orthogonal Functions. Astron. Astrophys., 1984, in press.
4. Wilson, R. M.: Sunspot Variation and Selected Associated Phenomena: A Look at Solar Cycle 21 and Beyond. NASA Technical Memorandum 82474, Marshall Space Flight Center, Alabama, February 1982.
5. Wilson, R. M.: A Comparative Look at Sunspot Cycles. NASA Technical Paper 2325, Marshall Space Flight Center, Alabama, May 1984.
6. Wilson, R. M.: On Long-Term Periodicities in the Sunspot Record. NASA Technical Memorandum 86458, Marshall Space Flight Center, Alabama, July 1984.
7. Waldmeier, M.: The Sunspot-Activity in the Years 1610-1960. Schulthess and Co., Zurich, Switzerland, 1961.
8. Eddy, J. A.: Climate and the Changing Sun. Climatic Change, Vol. 1, 1977, pp. 173-190.
9. Eddy, J. A.: The Historical Record of Solar Activity. The Ancient Sun: Fossil Record in the Earth, Moon and Meteorites, edited by R. O. Pepin, J. A. Eddy, and R. B. Merrill, Geochimica et Cosmochimica Acta Supplement 13, Pergamon Press, New York, New York, 1980, pp. 119-134.
10. Eddy, J. A.: The Maunder Minimum: A Reappraisal. Solar Phys., Vol. 89, 1983, pp. 195-207.
11. Wilson, R. M.; Rabin, D.; and Moore, R. L.: "Bimodality of the Solar Cycle. Science, 1984, submitted.
12. Teuber, D. L.: 1984, private communication.
13. Sargent, H. H., III: A Prediction for the Next Sunspot Cycle. IEEE Vehicular Technology Conference, 1978, pp. 490-496.
14. Yoshimura, H.: The Solar-Cycle Period-Amplitude Relation as Evidence of Hysteresis of the Solar-Cycle Nonlinear Magnetic Oscillation and the Long-Term (55 Year) Cyclic Modulation." Astrophys. J., Vol. 227, 1979, pp. 1047-1058.
15. Otaola, J. A. and Zenteno, G.: On the Existence of Long-Term Periodicities in Solar Activity. Solar Phys., Vol. 89, 1983, pp. 209-213.

16. Holland, R. L. and Vaughan, W. W.: Lagrangian Least-Squares Prediction of Solar Flux ($\bar{F}_{10.7}$). *J. Geophys. Res.*, Vol. 89, 1984, pp. 11-16.
17. Xu Zhen-tao, Zhao Ai-di, Mei Yan-lin, and Guo Quan-shi: Long-Term Forecasting of Solar Activity. *Solar Terrestrial Predictions Proceedings* (ed., R. F. Donnelly), Vol. 1, Boulder, Colorado, August 1979, pp. 163-167.
18. Fairbridge, R. W. and Hameed, S.: Phase Coherence of Solar Cycle Minima over Two 178-Year Periods. *Astron. J.*, Vol. 88, 1983, pp. 867-869.
19. Jose, P. D.: Sun's Motion and Sunspots. *Astron. J.*, Vol. 70, 1965, pp. 193-200.
20. Gregg, D. P.: A Nonlinear Solar Cycle Model with Potential for Forecasting on a Decadal Time Scale. *Solar Phys.*, Vol. 90, 1984, pp. 185-194.
21. Wilson, R. M.; Reichmann, E. J.; and Teuber, D. L.: An Empirical Method for Estimating Sunspot Number. *Solar Terrestrial Prediction Workshop, 1984*, to be published in the proceedings.